

## New Materials for Controlling Water Inrush and Sealing Tunnel Karst Pipes

Zhenjun WANG<sup>1</sup>, Qingsong ZHANG<sup>2</sup>, Bing HUI<sup>1\*</sup>, Rentai LIU<sup>2</sup>, Daoguo TIAN<sup>3</sup>, Yueqi ZHAO<sup>4</sup>

<sup>1</sup> Shandong Transportation Research Institute, No. 1877 Gangxi Road, Jinan 250104, Shandong, China

<sup>2</sup> Institute of Geotechnical and Underground Engineering, Shandong University, No. 17923 Jingshi Road, Jinan 250061, Shandong, China

<sup>3</sup> Jinan HuangHe Road and Bridge Construction Group Co., Ltd, No. 5111 Aoti Middle Road, Jinan 250014, Shandong, China

<sup>4</sup> Jinan Quality Safety Engineering Testing Co., LTD, No. 14306 Jingshi Road, Jinan 250014, Shandong, China

<http://doi.org/10.5755/j02.ms.36078>

Received 16 January 2024; accepted 5 March 2024

Water inrush disasters in karst areas have caused great losses to underground engineering construction, so it is urgent to control water gushing disasters in karst pipelines. In this paper, solution polymerization is used to prepare a grouting and sealing expanded matrix material to control disasters. Noncovalent weak interactions were used to improve the surface properties of the expanded matrix material, the effects of the natural polymer content on the properties of the matrix material were studied, and a modified expanded matrix material with an optimal response rate was prepared. A cross-linked curing agent (CCA) was developed and synthesized, and a new cross-linked expansive grouting and sealing material (WIS grouting material) with various particle sizes was synthesized with noncovalent interactions such as hydrogen bonding, static electricity, van der Waals forces, etc. The results showed that a 4 % solution polymer content (accounting for the particle mass of the expanded matrix) was the optimal dosage, and the optimal ratio of the modified expansion matrix material to the crosslinking curing agent was 1:1. The early compressive strength exceeded 0.2 MPa, and the water absorption rate reached 170 times. There was a power function relationship between the water absorption rate and time, and the rate was controlled by adjusting the particle sizes. The mechanism through which the WIS grouting material underwent expansion and crosslinking was explained at the microscopic level. The gel formed in response to water resisted dispersion in dynamic water and rapidly sealed karst pipe water gushers. This paper proposes a novel approach to utilizing the expansion characteristics of polymer chemical synthetic materials for crosslinking to seal karst pipe water gushers, effectively addressing the issue of poor resistance to dynamic water dispersion in traditional grouting materials used in karst areas. These results provide a scientific basis for the development and application of new materials to control water inrush in karst pipes.

**Keywords:** karst pipe inrush water, WIS grouting material, modified design, swelling crosslinking.

### 1. INTRODUCTION

China has the world's largest karst area and the widest distribution. Due to karst development, the geological conditions are complex and changeable, and they induce geological disasters that pose substantial threats to engineering construction. Among them, water inrush disasters in karst areas have caused the greatest losses to underground engineering construction and have become a key issue restricting underground construction [1–3]; they often cause casualties and economic losses, damage to the hydrogeological environment and ground subsidence, and other potential hazards, such as secondary disasters [4–6]. As an effective means of filling and consolidating underground formations such as fractures and pores, grouting is often used to block water and strengthen the formation [7–13]. The continuous research on grouting materials has led to the realization of a transition from single material to composite material, and from inorganic materials such as cement to organic materials. As a result, an increasing number of dynamic water grouting materials are being applied in karst areas. Aiming at the hidden

complexity of water gushing disasters in karst areas, Jin Qing et al. developed a grouting sealing material for karst pipes based on cement water glass grout through theoretical analysis, laboratory tests, physical model tests and other means. By adjusting the amount of xanthan gum, the sealing performance of the new grouting material was comprehensively tested, and the feasibility of the grouting material was verified in combination with engineering applications [14]. Li et al. developed a new cement water glass grouting material to solve the problem of water gushing disasters in karst pipelines. Through the grouting sealing test, they studied the sealing effect of grouting material under different influencing factors and drew the following conclusions: when the proportion of the modified construction solid waste cement-water glass grouting material in liquid a and liquid b is 1:1 and the mixing amount of waste red brick powder is 40–60 %, the grouting sealing performance is the best [15]. Using cement, clay, metaaluminate, and lignin as raw materials, Zhang et al. conducted laboratory tests to develop a novel cement-based composite grouting material. They investigated the diverse

\* Corresponding author. Tel.: +0531-85903918; fax: +0531-85903918.  
E-mail address: [huibing@sdjtky.cn](mailto:huibing@sdjtky.cn) (B. Hui)

properties of the grouting materials under various proportions and successfully applied this material in water-rich karst environments [16]. The polymer grouting material developed by Li exhibits a water absorption rate exceeding 300 times, making it well-suited for addressing water gushing in karst pipes [17]. However, the initial and final setting times of traditional Portland cement grouting materials are too long, but they do not meet the requirements of rapid setting and early strength for grouting in moving water, and the stabilities are poor. Most organic grouting materials are difficult to gel, relatively expensive and pose risks to the environment [18–22]. In addition, the existing expansive polymer grouting matrix materials can effectively achieve water plugging in karst pipes. However, the dispersion of colloidal particles formed by water is excessively large, making them prone to dispersion during high-flow water gushers and exhibiting poor resistance to dynamic water dispersion. Therefore, in view of the problems with grouting treatments in moving water, it is urgent to develop new grouting and plugging materials for tunnel karst pipeline water inrush.

Using the characteristics of water inflow in karst areas, this paper analyses the existing characteristics of polymer-expanded matrix materials, improves the surface properties of the matrix materials with noncovalent weak interactions, analyses the mechanisms for performance improvement with natural polymer solutions of expanded matrix materials, and identifies modified expanded matrix materials with the best response rate. A cross-linked curing agent (CCA) was developed and synthesized to prepare a new cross-linked expanding grouting and plugging material (WIS grouting material) through noncovalent interactions with modified matrix materials containing different particle sizes via noncovalent interactions, such as hydrogen bonding, electrostatic interactions, van der Waals forces, etc.; additionally, macroscopic and microscopic characterization of the new plugging materials was carried out with indoor tests. These results provide a scientific basis for the application of new materials for water inrush plugging of karst pipelines.

## 2. MATERIAL RESPONSE MECHANISM

Water inrush in karst areas generates high pressures, large flow volumes and rapid flow rates [23]. Grouting and plugging expansion matrix materials are synthetic polymer materials, and the polymer network is a solid bundle before contact with water and does not contain ion pairs. When the material reacts with water, the hydrophilic groups in the molecular chains form hydrogen bonds, the hydrophilic groups begin to dissociate, ionization produces anions, and electrostatic repulsions between the ions stretch the polymer mesh bundle. Additionally, to maintain electrical neutrality, cations cannot diffuse to the external solvent, so there is an increase in the concentrations of movable cations in the resin network; this generates osmotic pressure inside and outside the network structure, and water penetrates into the network through osmotic pressure. During water absorption and expansion of the matrix material, the three-dimensional cross-linked network produces a mirroring elastic contraction force. With increased water absorption, the osmotic pressure difference inside and outside the

network tends toward zero, and with expansion of the network, the elastic contraction force increases and gradually counteracts the electrostatic repulsion of the anions. When this elastic contraction force is equal to the electrostatic repulsion of the anions, the water absorbed by the material reaches equilibrium, that is, the maximum amount of water is absorbed. After the expanded matrix material is modified, the water absorption capacity and response rate increase. Fig. 1 shows the expansion characteristics of the matrix material.

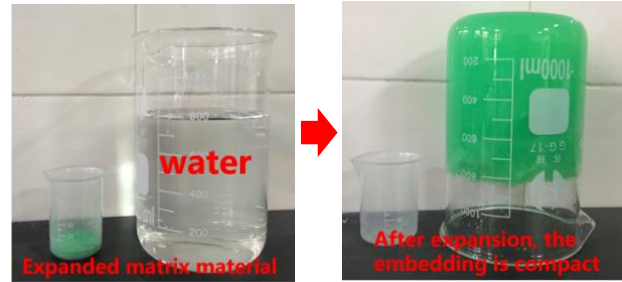


Fig. 1. Expansion of the matrix material

## 3. MATERIALS AND METHODS

### 3.1. Raw materials and test instruments

The expanded base material and natural polymer solution used in the development of WIS grouting materials need to be homemade, and the yellow dye is provided by Shanghai Meryer Chemical Technology Co., LTD. Crosslinking curing agent (CCA) is mainly prepared by analytical polyether PEG 2000 produced by Shanghai Macklin Biochemical Technology Co., Ltd., isocyanate TDI produced by Wanhua Chemical Group Co., Ltd., hydrophilic chain extender dimethylol propionic acid, neutralizing agent triethylamine, catalyst organotin, organic solvent acetone, etc. Raw materials and related test equipment are shown in Table 1 and Table 2.

Table 1. Raw materials and reagents

Raw materials	Specification	Manufacturer
Deionized water	–	Made by oneself
Natural polymer solution	–	Made by oneself
Expansion matrix material	0-0.6mm	Made by oneself
TDI	Industrial grade	Wanhua Chemical Group Co., Ltd.
Yellow dye	Guaranteed Reagent	Shanghai Macklin Biochemical Technology Co., Ltd.
Polyether PEG 2000	Analytical Reagent	Shanghai Macklin Biochemical Technology Co., Ltd.
Toluene	Analytical Reagent	Chinese medicine reagent
Acetone	Analytical Reagent	Chinese medicine reagent
Triethylamine	Analytical Reagent	Shanghai Macklin Biochemical Technology Co., Ltd.
Dimethylol propionic acid	Analytical Reagent	Shanghai Macklin Biochemical Technology Co., Ltd.
Organotin	Analytical Reagent	Shanghai Macklin Biochemical Technology Co., Ltd.

**Table 2.** Main experimental instruments and equipment

Name of instrument	Instrument model
Magnetic stirrer	—
Three-neck flask	—
Nitrogen protective cylinder	—
Tea bags	—
Thermometer	—
Rotary evaporator	N-1300D-WB
Vibrating screen machine	TG-TAM
Ultra-pure water machine	UPD-I-10TN
Universal testing machine	INSTRON-3344
Rheometer	HAAKE MARS40
Fourier transform infrared spectrometer	NEXUS 670
Thermogravimetric analyzer	SDT Q600 V20.9 Build 20
Scanning electron microscope	Hitachi S4800
Comminutor	KN-6788
Air blast drying oven	BPG-9040A

### 3.2. Modified design of the expansion matrix material

The reaction composite monomer AA/AM and deionized water were put into a beaker, a sodium hydroxide solution was added for neutralization, and quantitative amounts of redox initiators, cross-linking agents and yellow dyes were added for polymerization, and then the solid was dried at high temperature, crushed and screened to obtain the expanded matrix material. Then, the expanded matrix material was placed in the beaker as a control sample. Using the weak noncovalent interaction between the material and the natural polymer, a certain amount of the natural polymer solution was introduced on the surface of the expanded matrix material to crosslink the hydrophilic groups on the surface, and modification of the expanded matrix material was completed with granulation. Fig. 2 and Fig. 3 show the molecular structure of the preparation and modification of the expansion matrix material, respectively.

The effects of different polymer contents in solution on the water absorption rate of the modified expanded matrix material are shown in Fig. 4.

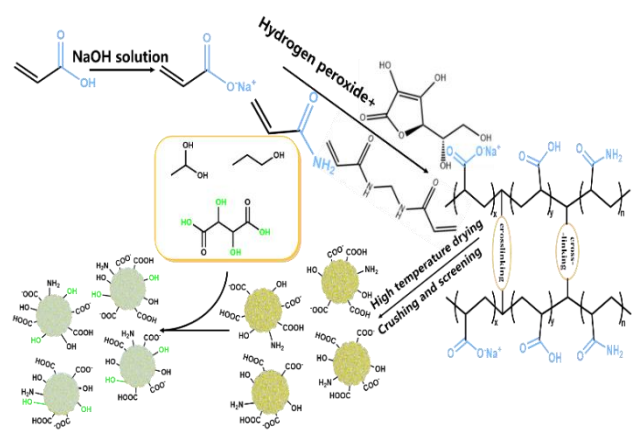
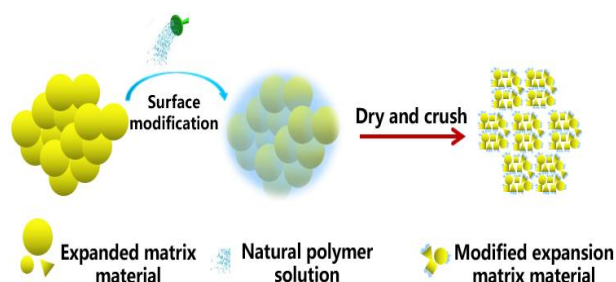
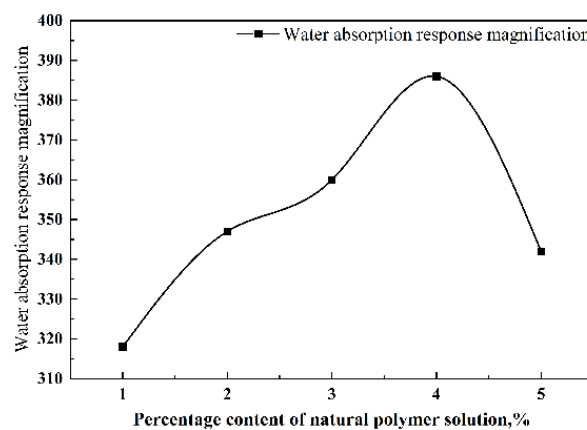
**Fig. 2.** Schematic diagram showing the molecular structure of the expansion matrix material and the synthetic route

Fig. 4. shows that when the content of the polymer solution (the mass of the solid particles in the expanded matrix) was less than 4 %, the water absorption rate of the modified material gradually increased with increasing

dosage, and when the content exceeded 4 %, the water absorption rate showed a decreasing trend, so the optimal dosage of the polymer in solution was 4 %, and the water absorption rate of the modified expanded matrix was 386 times.

**Fig. 3.** Schematic diagram showing modification of the expansion matrix material**Fig. 4.** Influence of the polymer content in solution on the water absorption rate

### 3.3. Preparation of the cross-linked curing agent (CCA)

A certain amount of polyether was weighed and placed in a rotary evaporator. The temperature was raised to 110 °C–120 °C, and the material was evacuated and dehydrated for 2 h until the water content was less than 0.05 %. The dehydrated polyether was added to a dry three-mouth bottle equipped with a magnetic mixer, the temperature was raised to 80 °C; the hydrophilic chain extender bis(hydroxymethyl)propionic acid and the acetone solvent were added under a nitrogen atmosphere, and isocyanate was slowly added dropwise after 1 h of reaction. The dropwise addition process was completed within 30 min. After that, the desired amount of the organotin catalyst was added to continue the reaction, an appropriate amount of acetone was added to reduce the solution viscosity, a neutralizing agent was added to the system solution with rapid magnetic stirring to provide an alkaline environment, and the organic solvent was removed after natural cooling to 65 °C to obtain the cross-linked curing agent (CCA).

### 3.4. Preparation of WIS grouting materials

The WIS grouting material is a functional polymer containing strongly hydrophilic groups and a cross-linking modified expansion matrix. To improve the mobility of the

material, anhydrous ethanol was introduced to enhance the fluidity of the material without affecting the properties of the grouting material. When preparing the WIS grouting material, the modified expanded matrix material was prepared as described above and put into the drying beaker. Then, an appropriate amount of the crosslinking curing agent CCA was added to a reaction vessel containing a diluent (anhydrous ethanol), and after stirring evenly, the modified expanded matrix material was added into the reaction vessel to prepare the WIS grouting material. Based on the complicated water absorption process of the modified expanded matrix material, the WIS grouting material was cross-linked to form discrete particles of the expanded matrix material through noncovalent interactions, such as hydrogen bonding, electrostatic and van der Waals forces, between the crosslinking curing agent and the modified matrix material with different particle sizes. In this process, CCA reacted with the functional groups of the modified expansive matrix material, and many hydrophilic cross-linking groups were introduced into the molecular chains of the CCA, which improved the surface activity of the material, and the cross-linked expansion reactions occurred in the presence of water to form agglutinative gels with hydrodynamic anti-dispersion ability. Fig. 5 contains a schematic diagram showing the preparation of the WIS grouting material:

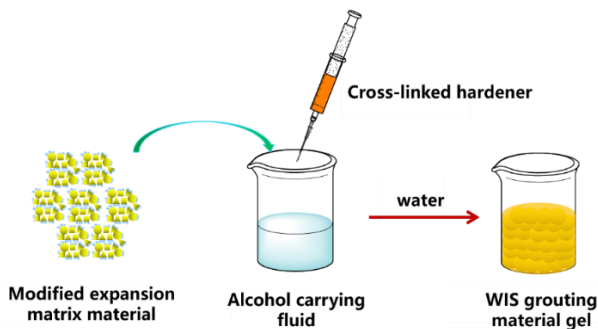


Fig. 5. Schematic diagram showing the preparation of the WIS grouting material

### 3.5. WIS grouting material performance tests

To provide a more comprehensive understanding of the properties and morphology of WIS grouting materials, a series of laboratory test methods were employed to conduct macroscopic testing and microscopic characterization. The macroscopic tests encompassed compressive strength and water response ratio evaluations, while the microscopic characterization involved SEM, FTIR, and TGA analyses [24].

#### 3.5.1. Compressive strength test

The rapid setting and early strength performance of grouting materials are widely considered as crucial indicators for evaluating the sealing effectiveness of grouting [25]. The strength of the WIS grouting material gel determined the plugging effect of the grouting material to a certain extent. Therefore, many experiments were performed to study and analyse the strengths of the materials, and the compressive strengths of the WIS grouting materials with various water absorption ratios were  $< 0.15$  mm,  $0.15$  mm  $< d < 0.3$  mm, and

$0.3$  mm  $< d < 0.6$  mm. The desired amount of WIS grouting material was poured into a 40 mm  $\times$  40 mm  $\times$  40 mm standard specimen mould, and then a certain amount of water was added and stirred until uniform to form a gel. A universal testing machine was used to test the compressive strengths of the solidified gel with different methods.

#### 3.5.2. Water absorption response ratio test

The efficient water absorption response of such grouting materials is believed by some researchers to be reflected in its ability to effectively reduce the flow velocity of moving water within the pipeline. This characteristic determines that its gel can partially obstruct the water channel, thereby achieving a state of "change to static" [26]. To measure the water absorption rates of the WIS grouting material, the modified material was screened, and material with particle sizes of  $d < 0.15$  mm,  $0.15$  mm  $< d < 0.3$  mm, and  $0.3$  mm  $< d < 0.6$  mm was used as the WIS grouting material. One gram was placed into a tea bag and immersed in water, and after the material reacted with water, the residual moisture on the surface was removed with filter paper, and the changes were recorded. The water absorption rate was calculated with Eq. 1.

$$Q = \frac{m_1 - m_0}{g} \quad (1)$$

where  $Q$  is the water absorption rate of the specimen;  $m_1$  is the total mass of the specimen after it was filled with water, g;  $m_0$  is the weight of the tea bag, g.

#### 3.5.3. SEM test

SEM was used to observe the structural morphology of the WIS grouting material in response to water, and then the consolidated body was placed in a freeze dryer for 24 hours. The liquid water was evacuated, frozen and sublimed to maintain the original form of the solid, and SEM was applied again. Additionally, SEM images of the expansion matrix, modified expansion matrix, CCA and modified expansion matrix gel after water absorption and lyophilization were used to compare the morphologies of each material.

#### 3.5.4. Infrared spectrum test

The sample to be measured was placed in the Fourier transform infrared-Raman spectrometer, and the spectrum was obtained over the range 4000  $\text{cm}^{-1}$  – 650  $\text{cm}^{-1}$ .

#### 3.5.5. Thermogravimetric test

The gel formed by the WIS grouting material with water was put into a lyophiliser for freeze-drying, and after 24 h, it was removed, formed into a block sample with a diameter of 3 mm and a height of 2 mm and put into a thermogravimetric analyser. Under a nitrogen atmosphere, the sample was heated from 30  $^{\circ}\text{C}$  to 790  $^{\circ}\text{C}$  at a rate of 10  $^{\circ}\text{C}/\text{min}$ .

## 4. RESULTS AND DISCUSSION

### 4.1. Compressive strength

The test data of compressive strength are shown in Table 3.

**Table 3.** Compressive strengths of grouting materials with different particle sizes and contents of the cross-linking curing agent

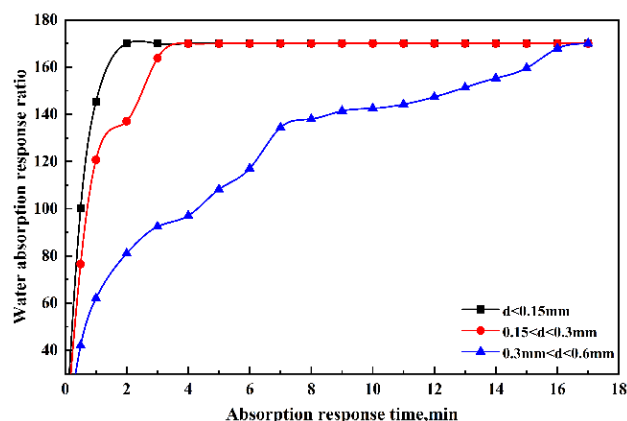
Particle size of the modified expanded matrix material, mm	WIS grouting material: water	Cross-linking curing agent content, %	Compressive strength, KPa
$d < 0.15$	1:5	30	99.86
	1:5	40	143.07
	1:5	50	220.68
	1:5	60	177.99
	1:5	70	151.97
	1:10	30	38.07
	1:10	40	55.26
	1:10	50	88.29
	1:10	60	46.18
	1:10	70	37.28
	1:15	30	11.27
	1:15	40	21.16
	1:15	50	34.09
	1:15	60	18.49
1:15	70	9.28	
$0.15 < d < 0.3$	1:5	30	99.33
	1:5	40	142.19
	1:5	50	219.03
	1:5	60	177.73
	1:5	70	151.27
	1:10	30	37.63
	1:10	40	54.88
	1:10	50	87.395
	1:10	60	45.22
	1:10	70	37.16
	1:15	30	10.26
	1:15	40	20.77
	1:15	50	33.95
	1:15	60	18.47
1:15	70	9.16	
$0.3 < d < 0.6$	1:5	30	99.24
	1:5	40	142.26
	1:5	50	218.86
	1:5	60	178.02
	1:5	70	150.28
	1:10	30	37.81
	1:10	40	55.02
	1:10	50	87.27
	1:10	60	45.37
	1:10	70	36.85
	1:15	30	10.17
	1:15	40	20.59
	1:15	50	33.83
	1:15	60	18.28
1:15	70	9.04	

Table 3 shows that the modified expansion matrix material formed with the addition of CCA as a cross-linking curing agent exhibited compressive strengths that first increased and then decreased as more CCA was added. With particle sizes  $d < 0.15$  mm, the strengths of the early gels exceeded 0.2 MPa when the ratio of modified expansion matrix material to CCA was 1:1. When the other ratios were constant, the compressive strengths of the gels formed with various particle sizes were comparable, which indicated that the modified expansion matrix materials with

different particle sizes required different times to reach the maximum water absorption rate. The compressive strengths for particle sizes  $d < 0.15$  mm were slightly larger, the particles were small, the particles per unit volume were more closely arranged, and the early plugging body formed after the material responded to water was more resistant to water pressure. However, Li's macroscopic performance test of grouting sealing materials did not include an investigation into the compressive strength performance, indicating a significant particle dispersion within the materials [17]. As a result, the newly developed grouting materials exhibit enhanced advantages. In the actual project, the modified expansion matrix material and a WIS grouting material with a ratio of 1:1 CCA should be selected to ensure that the plugging body formed has sufficient early strength to meet the needs of the grouting project.

#### 4.2. Water absorption response ratio

As shown in Fig. 6, as the CCA content of the crosslinking curing agent was increased, the water absorption rate of the WIS grouting material decreased slightly.



**Fig. 6.** Water absorption rates as a function of time

Fig. 7 shows that the time for WIS grouting materials with particle sizes  $d < 0.15$  mm to reach the maximum water absorption response rate was approximately 110 s, while the WIS grouting materials containing particle sizes of  $0.3 \text{ mm} < d < 0.6 \text{ mm}$  took approximately 17 min, so rates from 110 s to 17 min were controllable.

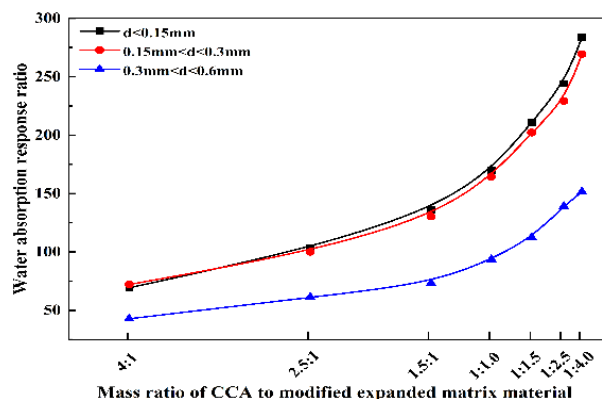


**Fig. 7.** Water absorption response time versus the CCA to modified expansion matrix ratio

When the particles were larger, the water absorption response rate was slower. The aforementioned rule aligns with previous research findings; however, the author's newly developed grouting material exhibits a superior water absorption response compared to Wang's studied material [27]. Consequently, the WIS grouting material possesses distinct advantages in tunnel karst engineering applications, and particle size can be tailored according to specific project requirements for effective water gusher sealing. The data in Fig. 7 were fitted with ORIGIN software to generate the following relationships:

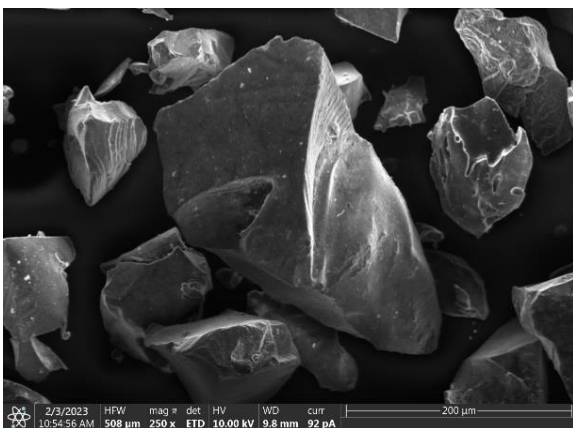
- 1) particle sizes  $d < 0.15$  mm:  $Q_t = 135.90t^{0.354}$ ;
- 2) particle sizes  $d < 0.15$  mm:  $Q_t = 109.44t^{0.340}$ ;
- 3) particle sizes  $0.3 \text{ mm} < d < 0.6$  mm:  $Q_t = 59.26t^{0.377}$ .

Note: these relationships use the time from the zero moment to the time when the material reaches the maximum water absorption response rate.

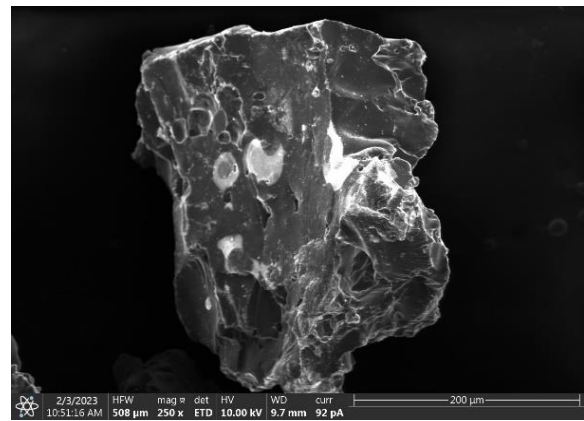
According to the above relationships, there was a significant power function relationship between the water absorption response and time.

### 4.3. SEM

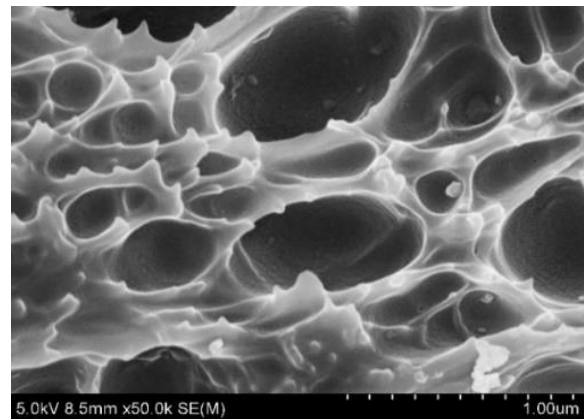
The morphological and structural characteristics of the expansion matrix, modified expansion matrix material and WIS grouting material are shown in Fig. 8 below. Fig. 8 a indicates the topography of the expansion matrix material. Cui's research findings indicate that the expanded matrix particles can directly and fully come into contact with water, resulting in the formation of a gel material [28]. The surface of the gel exhibits a folded structure, while each individual expanded matrix particle exists independently. However, when a large number of particles aggregate in water, they only loosely interact with each other without forming a cohesive whole due to poor hydrodynamic dispersion resistance caused by their viscosity against the karst pipe wall. Fig. 8 b shows the morphology of the modified expansion matrix material. The surface of the modified expansion matrix material had a very obvious fold structure, and this structure increased the contact area for the absorption of water. Fig. 8 c shows the morphology of the modified expanded matrix material after water absorption and freeze-drying, and the three-dimensional interpenetrating network structure of the modified expanded matrix material is clearly seen.



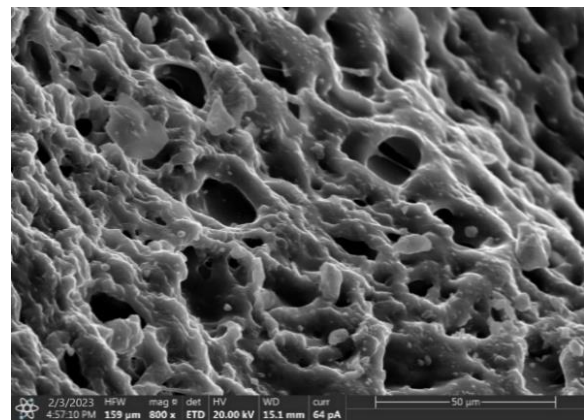
a



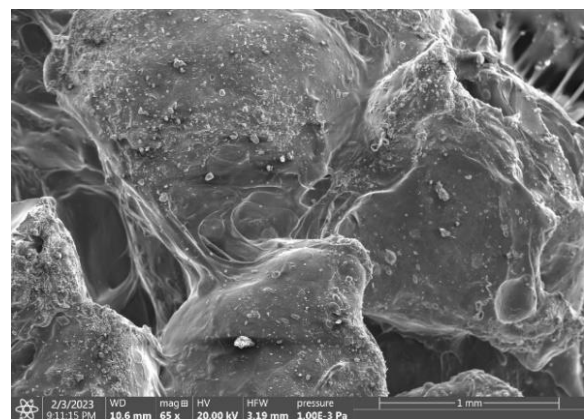
b



c

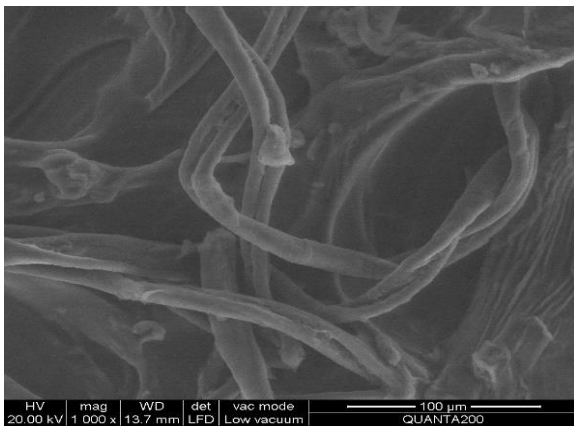


d



e

continued on next page



f

**Fig. 8.** Scanning electron microscopy images of the materials: a—the expansion matrix material; b—modified expanded matrix materials; c—modified expanded matrix material after water absorption and freeze-drying; d—the cross-linking curing agent CCA; e—the WIS grouting material is colloid after water absorption and freeze-drying; f—the WIS grouting material is colloidal after absorbing water

The molecular chains penetrated each other and were entangled to form the network structure, which increased the interaction strengths between the chains. After the three-dimensional cross-networked structure reacted with solvent water, the ion concentration inside the network was increased. Due to the osmotic pressure, the water penetrated the interior, the maximum water absorption rate was reached when the inside and outside pressures were balanced, and the modified expanded matrix material showed a significantly higher water absorption capacity.

Fig. 8 d shows the topography of the cross-linking curing agent CCA. There were many physical cross-linking points in the protruding part of the cross-linking curing agent, which increased the chain lengths and affected crosslinking after blending with the modified expansion matrix material. The rough surface of the CCA increased the contact area with the expansion matrix and enabled stronger adherence with the surface of the material, and the surface of the CCA had many hydrophilic groups that formed the cross-linked composite structure with the modified expanded matrix material.

Fig. 8 e shows the use of the modified expansion matrix material and cross-linked curing agent CCA to prepare the WIS grouting material that reacted with water to form a consolidated body and the freeze-dried cross-linked structural morphology. The cross-linked curing agent was attached to the surfaces of the particles of the modified expansion matrix material; the latter formed the core structure, and some of the crosslinking curing agents penetrated into the interior of the matrix material to form a dense mosaic structure. This mosaic composite structure underwent stacking so strong bonds were formed between the particles to improve adhesion of the material and form the new grouting material.

Fig. 8 f shows that the cross-linked WIS grouting material reacted with water to form a gel. In the presence of water, the crosslinking curing agent CCA was wrapped around the modified expanded matrix material, the gel was formed and stable crosslinking occurred, and the gel

exhibited an irregular pore-like structure that enhanced water absorption.

A comprehensive analysis of the morphological differences of materials under various states reveals that WIS grouting material incorporates the intricate fold structure and pore structure of modified expanded matrix material, effectively interconnecting loose matrix particles through cross-linking, and establishing contact with groundwater via a cross-linking curing agent CCA, which introduces numerous physical cross-linking points. As a result of this structurally induced cross-linking binding, water molecules gradually lose their mobility. The aqueous environment undergoes a transition from dynamic to static, thereby enabling the gel to exhibit an excellent water absorption response.

#### 4.4. Infrared spectrum

Fig. 9 shows the infrared spectra of the modified expansion matrix material, the CCA and the WIS grouting material. The characteristic peaks for the functional groups in the three materials were qualitatively analysed over time. The infrared spectrum of the WIS grouting material combined the basic spectral characteristics of the modified expansion matrix material and the CCA. The peak for the -NCO groups in the CCA material appeared at  $2265.5\text{ cm}^{-1}$  [29], but after blending with the modified expansion matrix material, the -NCO signal was absent from the spectrum of the WIS grouting material, which confirmed that the cross-linked hardener had reacted with the modified expansion matrix material. The modified expanded matrix material showed a carboxyl telescopic vibration peak at  $2865.5\text{ cm}^{-1}$ , and that peak was changed after the reaction, which also showed that crosslinking had occurred. It may be that the combination of the two materials increased the tension in the modified expansion matrix material, and the peaks for the WIS grouting material shifted. The WIS grouting material formed new cross-linked hydrophilic groups, which provided the cross-linked gel after reacting with water.

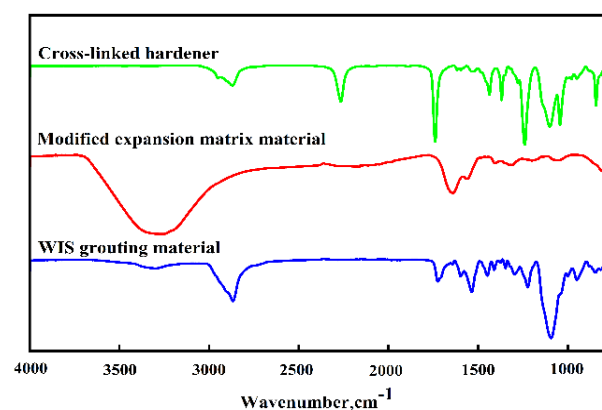


**Fig. 9.** Infrared spectra

#### 4.5. Thermogravimetric

Fig. 10 shows the thermogravimetric data for the gel formed by water and the WIS grouting material.

The data showed that the thermal decomposition process of the gel was roughly divided into the following stages. First, when the temperature rose from  $50\text{ }^{\circ}\text{C}$  to

215 °C, the water in the gel material evaporated, and small molecules were decomposed, resulting in a mass loss of 14.72 %. When the temperature was increased from 215 °C to 316 °C, the chemical bonds between molecules were broken, and the branched chains began to break, resulting in a mass loss of 13.64 %. When the temperature rose from 316 °C to 464 °C, the main chains of the gel material rapidly decomposed, and the functional groups began to dissociate, and the loss mass was 45.49 %, which was approximately half of the total mass. When the temperature increased from 464 °C to 800 °C, the residual monomer underwent decomposition, resulting in complete carbonization of the sample. At this stage, the mass began to stabilize and there was a significant slowdown in weight loss. The overall mass loss during this phase amounted to 14.35 %, with a final residue of ash measuring at 11.69 %. When the temperature reaches 100 °C, the gel experiences a weight loss of only 3.66 % [30]. Li's research findings demonstrate that the matrix material undergoes a colloidal weight loss of 5.24 % at this temperature, indicating that WIS grouting material is suitable for a wide range of temperatures and exhibits enhanced thermal stability during water flooding disaster control in karst areas [17].

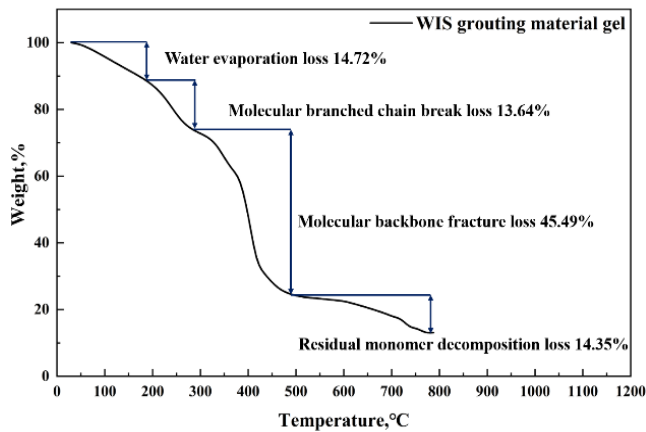


Fig. 10. Thermogravimetric analysis of the WIS gel

## 5. CONCLUSIONS

In this paper, water inrush characteristics in karst areas were considered to design the optimal grouting and sealing expansion matrix material. Based on noncovalent weak interactions between the natural polymer and the expansion matrix material, the effects of solutions with different polymer contents on the water absorption response rate were studied. The 4 % polymer solution (based on the particle mass of the expanded matrix) was deemed optimal.

At the macroscopic level, the optimal ratio of the modified expansion matrix material and the CCA was 1:1, the early compressive strength was greater than 0.2 MPa, and the water absorption rate was 170 times. There is a power function relationship between the water absorption rate and time, and the water absorption rate was controlled by adjusting the particle sizes.

At the microscopic level, the mechanism for expansion and crosslinking of the WIS grouting material was elaborated, new cross-linked hydrophilic groups were synthesized, and the gels formed in response to water showed good hydrodynamic resistance and facile

dispersion, so they quickly stopped water inrush in karst pipelines. The WIS grouting material is both environmentally friendly and non-toxic, ensuring zero environmental pollution.

This paper proposes a novel approach of utilizing the expansion characteristics of polymer chemical synthetic materials for crosslinking to seal karst pipe water gushers, effectively addressing the issue of poor resistance to dynamic water dispersion in traditional grouting materials used in karst areas. The research findings serve as a scientific basis for promoting and applying new materials for controlling water gushing in karst pipes.

## REFERENCES

1. **Zheng, Y.C., He, S.Y., Yu, Y., Zheng, J.Y., Zhu, Y., Liu, T.** Characteristics, Challenges and Countermeasures of Giant Karst Cave: A Case Study of Yujingshan Tunnel in High-Speed Railway *Tunnelling and Underground Space Technology* 114 2021: pp. 103988. <https://doi.org/10.1016/j.tust.2021.103988>
2. **Lin, C.J., Zhang, M., Zhou, Z.Q., Li, L.P., Shi, S.S., Chen, Y.X., Dai, W.J.** A New Quantitative Method for Risk Assessment of Water Inrush in Karst Tunnels Based on Variable Weight Function and Improved Cloud Model *Tunnelling and Underground Space Technology* 95 2020: pp. 103136. <https://doi.org/10.1016/j.tust.2019.103136>
3. **Liu, N., Pei, J.H., Cao, C.Y., Liu, X.Y., Huang, Y.X., Mei, G.X.** Geological Investigation and Treatment Measures Against Water Inrush Hazard in Karst Tunnels: A Case Study in Guiyang, Southwest China *Tunnelling and Underground Space Technology* 124 2022: pp. 104491. <https://doi.org/10.1016/j.tust.2022.104491>
4. **Shi, S.S., Guo, W.D., Li, S.C., Xie, X.K., Li, X.S., Zhao, R.J., Xue, Y., Lu, J.** Prediction of Tunnel Water Inflow Based on Stochastic Deterministic Three-Dimensional Fracture Network *Tunnelling and Underground Space Technology* 135 2023: pp. 104997. <https://doi.org/10.1016/j.tust.2023.104997>
5. **Li, S.C., Zhang, J., Li, Z.F., Gao, Y.F., Qi, Y.H., Li, H.Y., Zhang, Q.S.** Investigation and Practical Application of a New Cementitious Anti-Washout Grouting Material *Construction and Building Materials* 224 2019: pp. 66–77. <https://doi.org/10.1016/j.conbuildmat.2019.07.057>
6. **Hou, K., Wang, S., Yao, S., Niu, X.H., Li, Z., Wu, C.Q., Feng, G.R.** Research Progress on Modification of Polyurethane Grouting Materials in Mines *Coal Science and Technology* 50 (10) 2022: pp. 28–34. <https://doi.org/10.13199/j.cnki.cst.2021-0501>
7. **Li, S.C., Qi, Y.H., Li, Z.F., Li, H.Y., Zhang, J.** A Novel Treatment Method and Construction Technology of the Pipeline Gushing Water Geohazards in Karst Region *Tunnelling and Underground Space Technology* 113 2021: pp. 103939. <https://doi.org/10.1016/j.tust.2021.103939>
8. **Hang, C., Fu, J.Y., Yang, J.S., Ou, X.F., Ye, X.T., Zhang, Y.** Optimal Formulation Design of Polymer-Modified Cement Based Grouting Material for Loose Deposits *Construction and Building Materials* 261 (2) 2020: pp. 120513. <https://doi.org/10.1016/j.conbuildmat.2020.120513>
9. **Lin, C.J., Dai, W.J., Li, Z.F., Wang, Y.S.** Study on the Inorganic Synthesis from Recycled Cement and Solid Waste

- Gypsum System: Application in Grouting Materials *Construction and Building Materials* 251 2020: pp.118930. <https://doi.org/10.1016/j.conbuildmat.2020.118930>
10. **Wu, L.J., Wu, Z.J., Weng, L., Liu, Y., Liu, Q.S.** Investigation on Basic Properties and Microscopic Mechanisms of Polyacrylate Latex Modified Cement Grouting Material for Water Blocking and Reinforcement *Construction and Building Materials* 409 2023: pp. 133872. <https://doi.org/10.1016/j.conbuildmat.2023.133872>
  11. **Sha, F., Li, S.C., Liu, R.T., Li, Z.F., Zhang, Q.S.** Experimental Study on Performance Of Cement-Based Grouts Admixed With Fly Ash, Bentonite, Superplasticizer And Water Glass *Construction and Building Materials* 161 2018: pp. 282–291. <https://doi.org/10.1016/j.conbuildmat.2017.11.034>
  12. **Liu, J.Q., Yuen, K.V., Chen, W.Z., Zhou, X.S., Wang, W.** Grouting for Water and Mud Inrush Control in Weathered Granite Tunnel: A Case Study *Engineering Geology* 279 2020: pp. 105896. <https://doi.org/10.1016/j.enggeo.2020.105896>
  13. **Li, H., Yang, H.Q., Li, X.Y.** Investigation on the Working Performance of A Non-Dispersible Grouting Material for the Crack Repairment of Underwater Structures *Construction and Building Materials* 407 2023: pp. 133558. <https://doi.org/10.1016/j.conbuildmat.2023.133558>
  14. **Jin, Q., Qi, Y.H., Li, Z.F., Li, H.Y., Chen, J.P.** Research and Application of Modified Cement Grouting Materials for Gushing Water Disaster in Karst Conduit *Geotechnical and Geological Engineering* 40 (12) 2022: pp. 5855–5868. <https://doi.org/10.1007/S10706-022-02254-Y>
  15. **Li, H.Y., Zhang, Y.C., Wu, J., Zhang, X.Y., Zhang, L.W., Li, Z.F.** Grouting Sealing Mechanism of Water Gushing in Karst Pipelines and Engineering Application *Construction and Building Materials* 254 2020: pp. 119250. <https://doi.org/10.1016/j.conbuildmat.2020.119250>
  16. **Zhang, C., Yang, J.S., Fu, J.Y., Ou, X.F., Xie, Y.P., Dai, Y., Lei, J.S.** A New Clay-Cement Composite Grouting Material for Tunnelling in Underwater Karst Area *Journal of Central South University* 26 (07) 2019: pp. 1863–1873. <https://doi.org/10.1007/s11771-019-4140-5>
  17. **Li, S.C., Ma, C.Y., Liu, R.T., Chen, M.J., Yan, J., Wang, Z.J., Duan, S.L., Zhang, H.S.** Super-absorbent Swellable Polymer as Grouting Material for Treatment of Karst Water Inrush *International Journal of Mining Science and Technology* 031 (005) 2021: pp. 753–763. <https://doi.org/10.1016/j.ijmst.2021.06.004>
  18. **Su, T., Kong, X.M., Tian, H.W., Wang, D.M.** Effects of Comb-Like PCE and Linear Copolymers on Workability and Early Hydration of a Calcium Sulfoaluminate Belite Cement *Cement and Concrete Research* 123 2019: pp. 105801. <https://doi.org/10.1016/j.cemconres.2019.105801>
  19. **Kang, Y.S., Geng, Z., Liu, Q.S., Liu, B., Zhu, Y.G.** Research progress on support technology and methods for soft rock with large deformation hazards in China *Rock Soil Mech* 43 (08) 2022: pp. 2035–2059. <https://doi.org/10.16285/j.rsm.2021.1926>
  20. **Zeng, Z.P., Song, X.Y., Sun, Y., Song, S.L., Lu, W., He, Z.L.** Microstructure and Mechanical Property of Polyurethane/Water Glass Grouting Materials during Curing Process *Chinese Journal of Materials Research* 36 (11) 2022: pp. 855–861. <https://doi.org/10.11901/1005.3093.2021.467>
  21. **Wu, L.J., Wu, Z.J., Weng, L., Liu, Y., Liu, Q.S.** Investigation on Basic Properties and Microscopic Mechanisms of Polyacrylate Latex Modified Cement Grouting Material for Water Blocking and Reinforcement *Construction and Building Materials* 409 2023: pp. 133872. <https://doi.org/10.1016/j.conbuildmat.2023.133872>
  22. **Cui, W., Huang, J.Y., Song, H.F., Xiao, M.** Development of Two New Anti-washout Grouting Materials Using Multi-way ANOVA in Conjunction with Grey Relational Analysis *Construction and Building Materials* 156 2017: pp. 184–198. <https://doi.org/10.1016/j.conbuildmat.2017.08.126>
  23. **Wang, Y.C., Zheng, S.H., Zhong, Z.B., Li, Y.B., Li, Z.Y.** Experimental Investigation on the Hydraulic Characteristics of Water Inrush in Deep Buried Filled Karst Conduit Considering the Permeability *Transportation Geotechnics* 43 2023: pp. 101115. <https://doi.org/10.1016/j.trgeo.2023.101115>
  24. **Wang, J.J., Wang, Y.L., Yu, J., Xu, L., Li, M.L., Cheng, J.H., Li, Z.** Effects of Sodium Sulfate and Potassium Sulfate on the Properties of Calcium Sulfoaluminate (CSA) Cement Based Grouting Materials *Construction and Building Materials* 353 2022: pp. 129045. <https://doi.org/10.1016/j.conbuildmat.2022.129045>
  25. **Chen, X.M., Wang, J., Jiao, H.Z., Yang, Z., Zheng, D.T., Sun, J.Y.** Study on Early Hydration Mechanism of Double-Liquid Grouting Material Modified by Composite Early Strength Agent *Materials* 16 (19) 2023: pp. 6475. <https://doi.org/10.3390/ma16196475>
  26. **Zhou, M.M., Li, S.C., Zheng, Z., Liu, R.T., Chen, M.J., Ma, C.Y.** Theoretical and Experimental Study on The Rheological Properties of WIS Grout and the Dispersion and Sealing Mechanism *International Journal of Mining Science and Technology* 32 (4) 2022: pp. 669–684. <https://doi.org/10.1016/j.ijmst.2022.05.005>
  27. **Wang, M., Huang, J.L., Wang, S.J., Zhou, Y.B.** Study on Comparison and Optimization of Super Absorbent Materials for Underground Grouting in Coal Mine *Coal Science & Technology Magazine* 43 (03) 2022: pp. 24–28. <https://doi.org/10.19896/j.cnki.mtkj.2022.03.005>
  28. **Cui, Y., Tan, Z.S., An, C.X.** Research and Application of Multi-Functional Acrylic Resin Grouting Material *Construction and Building Materials* 359 2022: pp. 129381. <https://doi.org/10.1016/j.conbuildmat.2022.129381>
  29. **Ramani, R., Alam, S.** Free Volume and Damping in a Miscible High Performance Polymer Blend Positron Annihilation Lifetime and Dynamic Mechanical Thermal Analysis Studies *Journal of Applied Polymer Science* 133 (6) 2016: pp. 42961–42970. <https://doi.org/10.1002/app.42961>
  30. **Tao, J.H., Zhang, W.X., Liang, L., Lei, Z.Q.** Effects of Eco-Friendly Carbohydrate-Based Superabsorbent Polymers on Seed Germination and Seedling Growth of Maize *Royal Society Open Science* 5 (2) 2018: pp. 171–184. <https://doi.org/10.1098/rsos.171184>

